

Quark mass variation constraints from Big Bang nucleosynthesis

Paulo F. Bedaque,¹ Thomas Luu,² and Lucas Platter^{3,4}

¹Maryland Center for Fundamental Physics Department of Physics, University of Maryland, College Park, Maryland 20742, USA

²N-Section, Lawrence-Livermore National Laboratory, Livermore, California 94551, USA

³Institute for Nuclear Theory, University of Washington, Seattle, Washington 98195, USA

⁴Fundamental Physics, Chalmers University of Technology, SE-41296 Göteborg, Sweden

(Received 22 December 2010; published 15 April 2011)

We study the impact on the primordial abundances of light elements created by a variation of the quark masses at the time of Big Bang nucleosynthesis (BBN). In order to navigate through the particle and nuclear physics required to connect quark masses to binding energies and reaction rates in a model-independent way, we use lattice QCD data and a hierarchy of effective field theories. We find that the measured ${}^4\text{He}$ abundances put a bound of $-1\% \lesssim \delta m_q/m_q \lesssim 0.7\%$ on a possible variation of quark masses. The effect of quark mass variations on the deuterium abundances can be largely compensated by changes of the baryon-to-photon ratio η . Including bounds on the variation of η coming from WMAP results and adding some additional assumptions further narrows the range of allowed values of $\delta m_q/m_q$.

DOI: [10.1103/PhysRevC.83.045803](https://doi.org/10.1103/PhysRevC.83.045803)

PACS number(s): 26.35.+c, 06.20.Jr, 14.65.-q, 21.45.-v

I. INTRODUCTION

In theories of physics beyond the standard model, the standard model parameters appear not as fundamental constants but as derived quantities. In many of those theories the possibility then arises that the values of the standard model “constants” can vary over time [1]. It is then important to understand which constraints the successes of standard cosmology—which assumes time-independent constants—imposes on this purported time variation. A natural place to look for a strong sensitivity to a variation of fundamental constants is Big Bang nucleosynthesis (BBN) since it satisfies two important criteria. First, BBN happened very early in the universe’s history, mostly when the universe was between 3 seconds and 3 minutes old. Second, not only is standard BBN understood at a few percent level but it is also very sensitive to microscopic parameters such as nuclear binding energies and reaction rates that are, themselves, very sensitive to certain standard model constants. It is no surprise then that BBN has been used in the past to study the variation of fundamental constants [2]. The purpose of the present paper is to explore the BBN constraints on the variation of the masses of the two lightest quarks, m_u and m_d .

The binding of nucleons into light nuclei during BBN proceeds through a number of reactions, some of which are in equilibrium with the expansion of the universe and some of which are not. After weak reactions like $p + e^- \leftrightarrow n + \bar{\nu}$ are no longer in equilibrium (i.e., weak freezeout), the ratio of neutrons to protons decreases due to neutron β decay. If the formation of light nuclei occurred in equilibrium, the most bound nuclei (among the light ones this is ${}^4\text{He}$) would form earlier and more abundantly. The formation of ${}^4\text{He}$ can, however, only occur after ${}^2\text{H}$, ${}^3\text{He}$, and ${}^3\text{H}$ have been formed, since multinucleon fusion reactions are essentially impossible at the relatively low densities prevalent during BBN. Their number is small because their binding energies are small and it is not energetically favorable for them to form until the temperature is low enough to be comparable to their binding energies. Thus, the beginning of nucleosynthesis is delayed by the shallowness of the deuteron binding energy;

the so-called deuteron bottleneck. Since this shallowness is a product of delicate cancellations between kinetic and potential energies, the binding of the deuteron is an obvious place where a small change in quark masses can significantly alter the primordial abundances. Notice that the rate for the reaction $n + p \leftrightarrow d + \gamma$ is not small; it is sufficient to keep the deuteron number in thermal and chemical equilibrium. It is the equilibrium deuteron number that is too small for them to collide and be assembled in larger nuclei. After the deuteron number grows enough, the reactions leading to the formation of ${}^4\text{He}$ proceed quickly, and essentially all the neutrons present in the beginning of BBN are assembled into ${}^4\text{He}$ nuclei. The timing where this assembly starts (determined, among other things, by the deuteron binding) is crucial as the neutron numbers are decreasing due to neutron β decay. Small amounts of ${}^2\text{H}$, ${}^3\text{He}$, and ${}^3\text{H}$ are left out of this process. Their numbers depend critically on chemical nonequilibrium physics and the rates of the reactions, including the initial $n + p \rightarrow d + \gamma$ reaction. Current observation is not useful in measuring reliably the primordial abundance of ${}^3\text{He}$ and ${}^3\text{H}$. However, the abundance of ${}^2\text{H}$ and, especially, ${}^4\text{He}$ are well measured and put a significant constraint on any change of the standard BBN scenario.

A number of authors have previously considered the effect of quark mass variations on the BBN predicted abundances [3–15]. The main difficulty to be surmounted is that the quark mass dependence of binding energies, reaction cross sections, and decay rates that are input to BBN models are difficult to determine. For instance, modern nuclear potentials can describe very well nucleon-nucleon phase shifts. They can also be used to compute binding energies with enough precision (with the help of phenomenologically motivated three-nucleon forces fit to some observables) and cross section for few-nucleon reactions. These potentials are, however, tuned to data obtained from experiments where the quark mass has its current value. What is usually done in estimating the effect of quark mass variation is to change the parameters in these models where this dependence is easy to track. For instance, the range of nuclear forces, given by $1/m_\pi$, can be changed through the relation $m_\pi^2 \sim m_q$. However, the long-distance



FIG. 1. Strategy used to determine quark mass dependence of BBN abundances. At the far left, empirically determined LECs are used to constrain χ EFT, allowing predictions of nuclear observables and determination of their quark mass dependence. This theory is in turn matched onto the pionless EFT, where subsequent calculations of binding energies and reactivities relevant to BBN are used as input into BBN codes.

part of the potential, sensitive to this range, is actually a small part of the nucleon-nucleon interaction. The medium- and short-range parts also have a quark mass dependence and, while this dependence is likely to be milder, its effect on the overall nucleon-nucleon interactions is still large due to fine-tuned cancellations that are responsible for, among other things, the shallowness of the deuteron. In this paper we avoid, as much as possible, model-dependent approximations of the properties of nucleons and its nuclear forces, relying solely on the symmetries of QCD and its connection to nuclear physics through more general arguments. In particular we use effective field theories (supplemented with lattice QCD data) to connect the change in quark masses to the inputs used in BBN simulations.

A. Effective field theories

At momentum scales Q below $\Lambda_{\text{QCD}} \approx 1$ GeV, the relevant degrees of freedom in QCD are hadrons, not quarks and gluons. Effective field theories (EFTs) for this momentum range (i.e., chiral perturbation theory) were developed for the meson, one-, and many-nucleon sectors. They are able to predict physical observables as an expansion in the small parameters Q/Λ_{QCD} and $m_\pi/\Lambda_{\text{QCD}}$, taking as inputs a few “low-energy constants” (LECs), like pion decay constants and the nucleon mass in the chiral ($m_\pi = 0$) limit. These LECs, in turn, are determined from analyses of experimental results. Effective field theories predict, for example, the dependence of nucleon masses on the value of the quark masses. This particular change, however, is very small and can be neglected, except for its effect on the phase space for the neutron decay and related weak processes (see below). Lattice QCD calculations reinforce the belief in a small quark mass dependence of nucleon masses [16,17]. On the other hand, chiral perturbation theory for few-nucleon systems (referred to here as χ EFT) is in a less developed phase. First, there are conceptual issues that preclude a reliable prediction of the quark mass dependence of few-nucleon observables [18]. Second, it has not been used extensively in multinucleon systems and their reactions involving photons. To bypass this difficulty we use a low-energy effective theory where all particles, such as the pions, have been integrated out, leaving only the nucleon, photon, and neutrino degrees of freedom. Known as “pionless EFT,” the momentum scales Q relevant to this effective theory are much smaller than the pion mass m_π . This theory can make nontrivial predictions because the states pertinent to BBN (${}^2\text{H}$, ${}^3\text{He}$, ${}^4\text{He}$) are loosely bound and the typical momenta Q of their constituents are significantly below $\sim m_\pi$ and therefore within the regime of validity of the pionless EFT.¹ The

pionless EFT is very successful in predicting observables in the three-nucleon sector and there is an indication that the same is true in the four-nucleon sector [19,20]. Since the α particle is the most strongly bound of s -wave nuclei, its successful description in the pionless EFT might indicate that the theory can be useful in studying larger nuclei. Since the pionless EFT makes no use of the QCD chiral symmetry, it cannot directly predict the quark mass dependence of observables. The parameters of the pionless EFT, at the lowest orders in the low-energy expansion, are the threshold nucleon-nucleon scattering parameters (e.g., scattering lengths, effective ranges, etc.). These few parameters have been studied using χ EFT and we can use them to predict their variation with quark masses. In addition, some lattice QCD results confirm and reinforce the χ EFT predictions for scattering length dependencies on quark masses. We use these χ EFT results as input parameters for the pionless EFT. This allows us to obtain estimates for the quark mass dependence of nuclear properties relevant to BBN. We will then use this information in combination with a standard BBN code to compute the light element abundances in order to constrain the values of the quark masses during the universe’s first minutes. Our strategy of combining these two types of effective theories is summarized in Fig. 1. We will now describe the stages of our calculation.

B. Scattering length dependence on quark masses

Different versions of χ EFT have been used by different authors to study the quark mass variation of the nucleon-nucleon s -wave scattering lengths. The results depend on the spin channel. In the spin singlet 1S_0 channel and at leading order (LO) on the $m_\pi/\Lambda_{\text{QCD}}$ expansion, the calculation of the quark mass dependence of the scattering length in the version of χ EFT used in [21] requires as inputs the chiral limit values of the axial charge of the nucleon g_A , the decay constant of the pion f_π , the nucleon mass M , the pion mass m_π , and the coefficient of a two-nucleon contact term C_s^0 fitted to the physical scattering length. Only the value of these quantities at the physical value of quark masses is precisely known, but the difference between them and their chiral limit values is a higher-order effect that can be neglected in a next-to-leading order (NLO) calculation. At NLO a new constant D_s^2 appears (which is the coefficient of a two-nucleon operator with no derivatives but one quark mass insertion) as well as other constants contributing to the quark mass dependence of f_π, g_A , and M . The value of D_s^2 is difficult to disentangle from C_s^0 as both contribute equally to

¹The shallowness of these bound states is related to the fine tuning in the s -wave two-nucleon scattering. In fact, the scattering

length in the two spin channels 1S_0 and 3S_1 ($a_s \approx -22$ fm and $a_t \approx 5.4$ fm, respectively) are unnaturally large, much larger than the naive expectation $\approx 1/m_\pi = 1.4$ fm.

nucleon-nucleon scattering at the physical value of the quark masses. They give, however, different extrapolations to other values of quark masses. They can be disentangled only through a study of processes like deuteron-pion scattering or by the use of lattice QCD data (see below). The strategy used in dealing with the lack of knowledge of the value of D_s^2 is to estimate it using naive dimensional analysis arguments. In Ref. [21] D_s^2 was constrained by requiring its absolute value to be not too much larger than $|C_s^0|$ while in Ref. [22] D_s^2 itself was required to be of natural size. Fortunately, the difference in the power counting schemes used in [21] and [22] has little impact on the dependence of the scattering length on the quark masses, and the discrepancy between them can be explained by the different assumptions about the reasonable range of values for D_s^2 . We will use the calculation described in [22] as those authors computed the quark mass dependence of both the deuteron binding energy and nucleon-nucleon scattering lengths, since the deuteron binding energy is one of the most important ingredients in the BBN calculation.

For a small variation of the quark mass we can read the slope off Fig. 12 in Ref. [22] (we use the more conservative estimate where the change of the axial constant g_A with quark masses, parametrized by \bar{d}_{16} , is included):

$$\frac{m_q}{B_2} \frac{\delta B_2}{\delta m_q} = \frac{m_\pi}{2B_2} \frac{\delta B_2}{\delta m_\pi} = \frac{m_\pi}{2B_2} (-0.085 \pm 0.027), \quad (1.1)$$

where m_q is the average mass of the up and down quarks and we made use of the relation $m_\pi^2 \sim m_q$. Similarly, we use Fig. 12 in [22] to extract the variation of the spin singlet 1S_0 channel scattering length to find

$$\frac{\delta a_s}{\delta m_\pi} = \frac{2m_q}{m_\pi} \frac{\delta a_s}{\delta m_q} = (-1.4 \pm 1.4) \frac{\text{fm}}{\text{MeV}}. \quad (1.2)$$

Notice that a vanishing a_s variation is consistent with these extrapolations, a feature also seen in the extrapolation in [21]. If a_s were the only parameter determining the change of abundances due to varying quark masses, BBN would impose no constraint on possible quark mass variations.

Fully dynamical lattice QCD calculations of the nucleon-nucleon scattering lengths have appeared in the last few years. They are still performed at higher values of quark masses—too high for the effective theory approach to be valid—so they are of limited value for our purposes. Despite that, an attempt was made in [23] to use χ EFT to find the quark mass dependence of scattering lengths by interpolating the lowest pion mass lattice data and the known experimental value of the scattering lengths at the physical point. At this point in time, the deuteron binding energy has not been measured from lattice QCD. However, it is related, at leading order in the effective theory, to the triplet scattering length that is measured. Using the extrapolation in [23] and the leading order relation $B_2 = 1/(Ma_2^2)$ we find

$$\frac{m_q}{B_2} \frac{dB_2}{dm_\pi} = -0.14 \pm 0.13, \quad (1.3)$$

in agreement with Eq. (1.1). In the extrapolation done in [23] another branch of allowed values of dB_2/dm_π appears. This additional band is excluded from the purely EFT extrapolations in [21] and [22] and will be disregarded in this paper.

The allowed values for the a_s quark mass dependence extracted from the extrapolation in [23], namely

$$\frac{da_s}{dm_\pi} = (-0.75 \pm 1.0) \frac{\text{fm}}{\text{MeV}}, \quad (1.4)$$

are consistent with the ones above but are too loose to add any relevant constraint.

The remaining inputs of the pionless EFT, like three-nucleon interaction parameters, effective ranges, nucleon magnetic moments, etc., are not fine tuned and therefore vary much less drastically with the quark masses. Their contribution to the overall fusion cross sections is also suppressed compared to B_2 and a_s . In the present paper we will take them to be independent of the quark masses.

C. Binding energies, reactivities, and lifetimes

We have used the pionless EFT to estimate the quark mass variation of four quantities: the binding energies of the deuteron, ^3H , ^3He , and ^4He and the reactivity of the process $n + p \rightarrow d + \gamma$. Similar calculations were carried out for ^3H in the context of infrared limit cycles in Refs. [24–26]. The binding energies of larger nuclei, like ^7Li , are important only for the abundances for these larger nuclei. As it is not presently possible to have a reliable estimate on the quark mass variation of these binding energies, we keep them fixed and concentrate on the abundances for the lighter nuclei ^2H and ^4He , confident that they will not be significantly affected by the binding of $A > 4$ nuclei. We also only include the variation of the reactivity of proton-neutron capture as this is the reaction that initiates BBN and is more likely to have an impact on abundances (but, as we will see below, this impact is minimal). The binding energy of the deuteron is given by Eq. (1.1).

The calculation of three-nucleon and four-nucleon properties in the pionless EFT requires as inputs the singlet and triplet scattering lengths as well as one three-body observable, usually taken to be the triton binding energy. This binding energy can be traded by the value of a three-body force counterterm. The three-body force is also not fine tuned and will therefore show only a weak dependence on the quark masses that we will consequently neglect. Changing the two-body input while keeping the three-body counterterm fixed provides then the scattering length dependence of the three-nucleon system. In other words, the binding energies of the ^3He , ^3H , and ^4He nuclei are estimated by

$$\frac{m_q}{B_i} \frac{dB_i}{dm_q} = \frac{m_q}{B_i} \left(\frac{da_s}{dm_q} \frac{dB_i}{da_s} + \frac{dB_2}{dm_q} \frac{dB_i}{dB_2} \right), \quad (1.5)$$

where B_i stands for the binding energy of one of ^3He , ^3H , or ^4He . The values of the derivatives appearing in Eq. (1.5) were computed using the pionless EFT:

$$\frac{a_s}{B_3} \frac{dB_3}{da_s} = 0.12, \quad \frac{B_2}{B_3} \frac{dB_4}{dB_2} = 1.41, \quad (1.6)$$

$$\frac{a_s}{B_4} \frac{dB_4}{da_s} = 0.037, \quad \frac{B_2}{B_4} \frac{dB_4}{dB_2} = 0.74, \quad (1.7)$$

where B_4 is the ^4He binding and B_3 is the ^3H or ^3He binding energy. The weak dependence on a_s is easily understood when one notices that the typical momentum in these bound states

is of order $\sqrt{MB_i}$, which is much larger than $1/a_s$. The dependence of B_i on a_s is a function of the dimensionless parameter $\sim\sqrt{MB_i}a_s \ll 1$ and therefore taken to be zero.

In order to account for the theoretical uncertainty in the EFT calculation we assign an additional 10% random variation to the bindings of ${}^3\text{He}$ and ${}^3\text{H}$ (computed at NLO in EFT) and a 30% variation on the value of the ${}^4\text{He}$ binding (computed at LO only), as will be shown more explicitly below.

The reaction $n + p \leftrightarrow d + \gamma$ was extensively analyzed in Ref. [27] using an N^4 LO calculation in the pionless EFT. The inputs at this order are the scattering length a_s , the deuteron binding energy, the corresponding effective range parameters, the magnetic moments of the deuteron, and a single two-nucleon-one-photon term fixed by experiment. We use the variation of B_2 and a_s given in Eqs. (1.1) and (1.2) to compute, with the help of the explicit formula in [27], the relative change in the reactivity as a function of the temperature and use this as input for the BBN code. In [4] it was argued that the reactivity $\langle\sigma v\rangle$ scales as $\sim B_2^{5/2}a_s^2$. We verified with the explicit formula from [27] that the scaling with $B_2^{5/2}$ is indeed very well satisfied but that the scaling with a_s^2 does not work as well.

Finally, we discuss how quark mass changes affect the neutron lifetime as well as the rates of other one-baryon weak reactions such as $p + e^- \leftrightarrow n + \nu$. This effect arises from a modified value of the axial charge g_A and the neutron and proton masses, which in turn dictate the allowed kinematic phase space for these weak reactions. In fact, the neutron width is given by [28]

$$\Gamma = \frac{(G_F \cos \theta_C)^2}{2\pi^3} m_e^5 (1 + 3g_A^2) f\left(\frac{\Delta}{m_e}\right), \quad (1.8)$$

where $\Delta = m_n - m_p$ and m_e are the mass splitting between neutron and proton and the electron mass, respectively, $g_A \approx 1.26$ is the nucleon axial decay constant, G_F is the Fermi constant, and θ_C is the Cabibbo angle. The function $f(\Delta/m_e)$ is

$$f(w_0) = \int_1^{w_0} dw w \sqrt{w^2 - 1} (w_0 - w)^2 \frac{2\pi\alpha}{\sqrt{w^2 - 1}} \frac{1}{1 - e^{-\frac{2\pi\alpha}{\sqrt{w^2 - 1}}}}, \quad (1.9)$$

which describes the phase space and the Coulomb repulsion. The variation of Γ with the quark masses is given then by

$$\frac{m_q}{\Gamma} \frac{d\Gamma}{dm_q} = \frac{m_q}{f\left(\frac{\Delta}{m_e}\right)} \frac{d}{dm_q} f\left(\frac{\Delta}{m_e}\right) + \frac{m_q}{1 + 3g_A^2} 3 \frac{d(g_A^2)}{dm_q}. \quad (1.10)$$

The dependence of g_A with the quark mass is given, at NLO in chiral perturbation theory, by [29]

$$g_A = g_A^0 \left[1 - \frac{9g_A^2 m_\pi^2}{32\pi^2 F^2} \ln\left(\frac{m_\pi}{\Lambda}\right) + \frac{(g_A^2 - 4)m_\pi^2}{32\pi^2 F^2} \ln\left(\frac{m_\pi}{\Lambda'}\right) \right], \quad (1.11)$$

where g_A^0 is the chiral value of g_A , $F \approx 93$ MeV, and Λ and Λ' are constants of order 1 GeV dependent on the Gasser-Leutwyler coefficients [30]. Numerically we find

$$\frac{m_q}{1 + 3g_A^2} 3 \frac{d(g_A^2)}{dm_q} = \frac{1}{2} \frac{m_\pi}{1 + 3g_A^2} 3 \frac{d(g_A^2)}{dm_\pi} \approx 0.2. \quad (1.12)$$

The variation of the phase space $f(\Delta/m_e)$ with the quark masses can be estimated as

$$\begin{aligned} \frac{m_q}{f\left(\frac{\Delta}{m_e}\right)} \frac{d}{dm_q} f\left(\frac{\Delta}{m_e}\right) &= \frac{m_\pi}{2f\left(\frac{\Delta}{m_e}\right)} \frac{df\left(\frac{\Delta}{m_e}\right)}{dm_\pi} \\ &= \frac{m_\pi}{2f(w_0)} \frac{df(w_0)}{dw_0} \Big|_{w_0=\frac{\Delta}{m_e}} \frac{d\Delta/m_e}{dm_\pi}. \end{aligned} \quad (1.13)$$

The value of $f(w_0)$ and its derivative at $w_0 = \Delta/m_e$ is found numerically to be 1.64 and 4.25, respectively. The variation of Δ/m_e with m_q can be estimated by splitting Δ into a strong interaction component Δ_s proportional to the up and down quark mass difference (and, consequently, to the value of m_q) and an electromagnetic piece Δ_{EM} , largely independent of m_q . Unfortunately, the electromagnetic part is due to short distance effects and cannot be directly computed in a reliable way. The best handle we have on its value comes from chiral perturbation theory, where the up and down quark mass ratio, the meson spectrum, and the best estimate of the nucleon σ -term are used as inputs to extract Δ_s . The value obtained for Δ_s in this manner is consistent with that obtained from lattice QCD calculation [31]. The difference between this value of Δ_s and the measured value of the neutron-proton mass splitting gives $\Delta_{\text{EM}} = -0.76 \pm 0.30$ [32].

Chiral perturbation theory predicts a quark mass dependence of Δ_s of the form $\Delta_s = Am_\pi^2(m_d - m_u)/(m_d + m_u)$, a formula valid up to NLO since the leading order loop contribution to the nucleon mass cancels between the neutron and proton. We then have

$$\begin{aligned} \frac{m_q}{f\left(\frac{\Delta}{m_e}\right)} \frac{df\left(\frac{\Delta}{m_e}\right)}{dm_q} &= \frac{1}{f(w_0)} \frac{df(w_0)}{dw_0} \Big|_{w_0=\frac{\Delta}{m_e}} \frac{m_\pi}{2m_e} A \frac{m_d - m_u}{m_d + m_u} 2m_\pi \\ &= \frac{1}{f(w_0)} \frac{df(w_0)}{dw_0} \Big|_{w_0=\frac{\Delta}{m_e}} \frac{\Delta_s}{m_e} \\ &\approx 10.4 \pm 1.5. \end{aligned} \quad (1.14)$$

Notice that we are taking both the up and down mass to vary while keeping the ratio m_d/m_u fixed. As the dependence in Eq. (1.14) dominates over Eq. (1.12), we finally find

$$\frac{m_q}{\Gamma} \frac{d\Gamma}{dm_q} = 10.6 \pm 1.5. \quad (1.15)$$

The quark mass variation of the neutron lifetime is relevant for our calculation. In order to see that, let us remember that the neutron number, after the weak interactions are decoupled, decreases until BBN starts at $t \approx 168$ s. The suppression factor in standard BBN is thus $e^{-168/885} \approx 0.827$. A 5% increase of quark masses would lead, according to Eq. (1.14), to a decrease of about 50% in the neutron lifetime and the suppression factor would change to $e^{-252/885} \approx 0.752$, leading to a change of

about 10% in the ${}^4\text{He}$ abundance; a variation comparable to the observational uncertainties.

The rate of other weak reactions changes in a similar manner. The phase space integrals are more involved and are, in BBN codes, computed “on the fly,” taking the ratio $Q = \Delta/m_e$ as input. We calculated the variation of Q as

$$\begin{aligned} \frac{m_q}{Q} \frac{dQ}{dm_q} &= \frac{m_\pi}{2\Delta} \frac{d\Delta}{dm_\pi} = \frac{\Delta_s}{\Delta} \\ &\approx 1.59 \pm 0.23. \end{aligned} \quad (1.16)$$

II. RESULTS

In order to deal with the highly nonlinear dependence of the final abundances on the quark masses and, at same time, to include estimates of theoretical errors, we use a stochastic procedure. More specifically, for a given quark mass variation $\delta m_q/m_q$, we specify the binding energies of ${}^2\text{H}$, ${}^3\text{H}$, ${}^3\text{He}$, and ${}^4\text{He}$, the reactivity $\langle\sigma v\rangle$ for $n + p \leftrightarrow d + \gamma$, the neutron lifetime τ , and the phase space parameter Q . All other BBN parameters are kept at their present values.

We have randomly generated a set of 300 values of scattering lengths a_s and deuteron bindings B_2 with a Gaussian distribution with mean value and standard deviation given by

$$\begin{aligned} \bar{X} &= \left[1 + \frac{1}{2} \left(\left. \frac{m_q}{X} \frac{dX}{dm_q} \right|_+ + \left. \frac{m_q}{X} \frac{dX}{dm_q} \right|_- \right) \frac{\Delta m_q}{m_q} \right] X^{\text{phys}}, \\ \sigma_X &= \left[1 + \frac{1}{2} \left(\left. \frac{m_q}{X} \frac{dX}{dm_q} \right|_+ - \left. \frac{m_q}{X} \frac{dX}{dm_q} \right|_- \right) \frac{\Delta m_q}{m_q} \right] X^{\text{phys}}, \end{aligned} \quad (2.1)$$

where X stands for either a_s or B_2 and the “+” and “−” subscripts refer to the higher and lower values of dX/dm_q , respectively, allowed by Eqs. (1.1) and (1.2). The variations of a_s and B_2 are assumed to be uncorrelated. From the ensemble of a_s and B_2 obtained as above, we compute a corresponding ensemble of binding energies using Eq. (1.5) and add to the result a 10% (for ${}^3\text{H}$ and ${}^3\text{He}$) or 30% (for ${}^4\text{He}$) relative random error to take into account theoretical errors discussed in the previous section. The binding energies of ${}^3\text{H}$, ${}^3\text{He}$, and ${}^4\text{He}$ are then given by

$$\frac{B_i}{B^{\text{phys}}} = \left[1 + (1 + t_i \xi_i) \left(\frac{a_s}{B_i} \frac{dB_i}{da_s} + \frac{B_2}{B_i} \frac{dB_i}{dB_2} \right) (a_s - a_s^{\text{phys}}) \right], \quad (2.2)$$

where i indexes the three nuclei ${}^3\text{H}$, ${}^3\text{He}$, and ${}^4\text{He}$, the superscript “phys” stands for the present experimental values of the quantity, ξ_i are Gaussian random variables with central value 0 and standard deviation equal to 1, and t_i is the theoretical error of the extrapolation equal to 0.1 (for ${}^3\text{H}$ and ${}^3\text{He}$) and 0.3 (for ${}^4\text{He}$).

Similarly, the reactivity $\langle\sigma v\rangle_T$ of the $n + p \rightarrow d + \gamma$ reaction was computed as a function of the temperature T for the ensemble of $a_s B_2$ values determined by Eq. (2.1) using the explicit expression for the cross section from [27]. The high-order expansion of this calculation in [27] is accompanied with very small theoretical errors that we subsequently neglect.

We also generated, for each value of $\delta m_q/m_q$, a set of 300 random values of τ and Q whose distribution reflect the discussion in the previous section. More specifically, these values were generated through the formula

$$\begin{aligned} \frac{1}{\tau} &= \frac{1}{\tau^{\text{phys}}} \left[1 + (10.6 + 1.5\xi) \frac{\delta m_q}{m_q} \right], \\ Q &= Q^{\text{phys}} \left[1 + (1.59 + 0.23\xi) \frac{\delta m_q}{m_q} \right], \end{aligned} \quad (2.3)$$

where ξ is a Gaussian random variable with central value 0 and standard deviation 1. Notice that this ξ is independent of the ξ_i used in the determination of the binding energies but the same ξ is used in both τ and Q since the leading theoretical uncertainties on both quantities stem from the same determination of the σ -term.

For a given value of $\delta m_q/m_q$, a set of values for B_2 , $B_3\text{H}$, $B_3\text{He}$, B_4 , and $\langle\sigma v\rangle_T$ was paired to one of the set of τ and Q values and used in a standard BBN code. The BBN code we have used in our analysis is based on Refs. [33,34] and is publicly available [35]. The code was modified to accept temperature-dependent variations in the reactivity corresponding to the $n + p \rightarrow d + \gamma$ reaction and the rate of weak interaction processes was changed according to Eqs. (1.15) and (1.16). The Q values of all BBN reactions with ${}^2\text{H}$, ${}^3\text{H}$, ${}^3\text{He}$, and ${}^4\text{He}$ as either parent or daughter products of reactions were allowed to vary in accordance with the changes in binding energies of these nuclei. The baryon-to-photon ratio η was changed over a range discussed below. Otherwise, the standard input parameters were used in our BBN simulations.

The main feature seen in the simulations is that a variation in η shifts the deuterium abundance but has little effect on the ${}^4\text{He}$ yields [see Fig. 2]. A larger value of η implies, in a larger baryon density, a more complete burning of the neutrons into ${}^4\text{He}$ nuclei and a smaller deuterium abundance. As a consequence, in the absence of a restriction on the value of

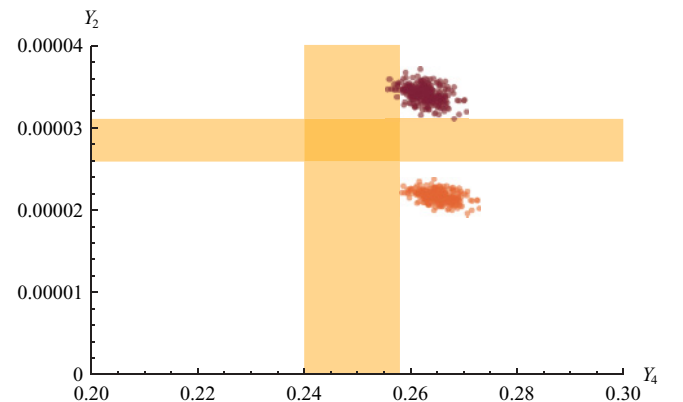


FIG. 2. (Color online) Yellow bands show the $1\text{-}\sigma$ allowed abundances for ${}^4\text{He}$ and ${}^2\text{H}$. The two clouds show the result of 300 simulations, both with $\Delta m_q/m_q = -1\%$ but two different values of η_{10} . The lower cloud (ochre) is the result of taking $\eta_{10} = 6.23$ and the upper cloud (burgundy) is the result of taking $\eta_{10} = 4.60$. There is very little change in the ${}^4\text{He}$ yield but the deuterium yield changes enough to render the deuterium abundance useless in putting a constraint on $\Delta m_q/m_q$.

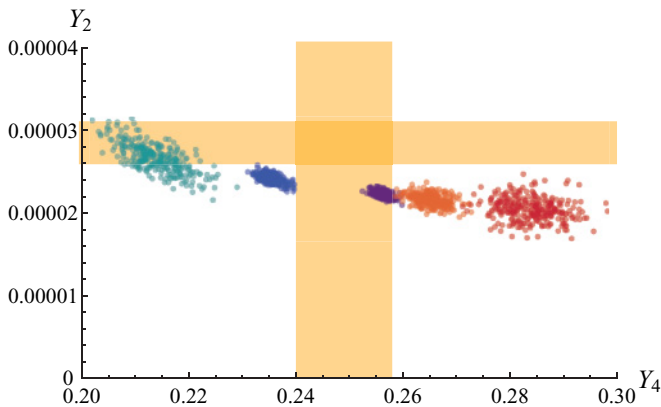


FIG. 3. (Color online) Yellow bands show the $1\text{-}\sigma$ allowed abundances for ${}^4\text{He}$ and ${}^2\text{H}$. The five clouds show the result of 300 simulations at each one of the values (from left to right): $\Delta m_q/m_q = 2\%$ (green), $\Delta m_q/m_q = 0.7\%$ (blue), $\Delta m_q/m_q = -0.5\%$ (purple), $\Delta m_q/m_q = -1\%$ (ochre), and $\Delta m_q/m_q = -2\%$ (red).

η from other considerations, the deuterium abundance does not put any constraints on the range of allowed quark mass variations.

Additional constraints on the value of η come from studies of the large-scale structure of the universe. The actual numerical value of the constraints, however, depends on assumptions made in these analyses, including assumptions on the initial spectrum of fluctuations. For instance, the lower range of the determination of $\eta_{10} = 4.79 \pm 0.019$ in [36] and the central value of the determination of $\eta_{10} = 6.23 \pm 0.17$ in [37] are shown for $\delta m_q/m_q$ in Fig. 2. A similar plot results from other values of $\delta m_q/m_q$. Consequently, any reasonable change in the deuterium abundance can be accommodated by a change in the value of η_{10} . If we restrict ourselves to the much narrower range $\eta_{10} = 6.23 \pm 0.17$ [37], the deuterium abundances can play a role. However, the values in the range $\eta_{10} = 6.23 \pm 0.17$ are in tension with the observed deuterium abundances. BBN, by itself, prefers the slightly lower range $5.1 < \eta_{10} < 6.5$ at the 95% confidence level [38]. Thus, even with the current physical values of m_q , the predicted deuterium abundance lies just outside the $1\text{-}\sigma$ band, making it difficult to distinguish the allowed and forbidden values of m_q based on Y_2 . Therefore, to proceed further, we disregard the deuterium abundances and look at how the ${}^4\text{He}$ abundances change with the quark masses.

In Fig. 3 we show the result of changing the quark masses by five values: 2%, 0.7%, -0.5% , -1% , and -2% , all corresponding to $\eta_{10} = 6.23$. Each one of these values of $\delta m_q/m_q$ is represented by a cloud of points in the $Y_4 \times Y_2$ plane. The spread between the 300 points in each cloud accounts for the theoretical uncertainties in the extrapolation of the parameter inputs as described by Eqs. (2.2) and (2.3). The tendency is for a smaller Y_4 for larger values of m_q . Two main mechanisms account for this general trend. First, large values of m_q imply larger values of Δ , as well as a larger phase space for neutron decay and therefore shorter neutron lifetime. Consequently, more neutrons decay by the time BBN starts the assembly of ${}^4\text{He}$, resulting in smaller ${}^4\text{He}$ yields. In addition, Eq. (1.1) shows that a larger m_q implies a smaller B_2 . The deuteron, being less bound, takes longer to form, delaying

the onset of ${}^4\text{He}$ formation and giving even more time for the neutrons to decay, reducing further the ${}^4\text{He}$ yields. There is also a weak tendency to have smaller Y_2 for smaller m_q , a trend not so easily explained.

Based on the data shown on Fig. 3 we put a bound on the allowed values of quark mass changes at

$$-1\% \lesssim \frac{\Delta m_q}{m_q} \lesssim 0.7\%, \quad (2.4)$$

which is the main result of this paper. We refrain from assigning a numerical value to the uncertainty in this estimate, as an attempt in this direction would require us to assign a precise statistical meaning to our theoretical uncertainties. While there are reasons to take these uncertainties seriously at the qualitative level, we believe them to be superior to the model calculations used previously.

III. CONCLUSION

We have estimated the abundances of ${}^2\text{H}$ and ${}^4\text{He}$ produced in the standard BBN scenario under the assumption that the light quark masses were shifted at the BBN time from their present values. In order to perform this calculation we have used input from several effective field theories as well as lattice QCD results to connect the quark mass variation to the relevant nuclear physics pertinent to BBN. We found that a variation beyond the $-1\% \lesssim \frac{\Delta m_q}{m_q} \lesssim 0.7\%$ range to likely be inconsistent with the observed abundances.

Two of the BBN parameters played the largest roles in changing the light element yields: the deuteron binding energy B_2 (with the ${}^3\text{H}$, ${}^3\text{He}$, and ${}^4\text{He}$ binding energies strongly correlated with B_2) and the neutron lifetime. The dependence of the neutron lifetime on the quark mass values is well constrained by theory. The variation of the deuteron binding is, however, much less constrained and several venues of further progress are clearly visible (for a very recent study, see [39]). Lattice QCD calculations of nucleon-nucleon interactions, even if performed at unphysical values of m_q , would go a long way in narrowing these constraints. As long as they are performed with quark masses low enough to be within the region of validity of the chiral nuclear EFT, they determine reliably the value of parameters of the EFT necessary for the extrapolation of the deuteron binding energy. The binding energies of ${}^3\text{H}$, ${}^3\text{He}$, and, especially, ${}^4\text{He}$ can and should be computed in the pionless nuclear EFT to higher orders so that theoretical uncertainties associated with these quantities decrease. Finally, a better understanding of the quark mass variation of other threshold parameters like effective ranges, magnetic moments, etc., would also allow for a more precisely constrained calculation of the binding energies on nuclei larger than ${}^4\text{He}$.

A number of other works have also considered the effects of a variation of the quark masses on properties of light nuclei. For example, in Ref. [8] this effect was implemented by a change of the pion mass in the phenomenological model interaction employed in the calculations. Such an interaction is only able to capture the true quark mass dependence to a limited degree since it is not constructed as a systematic expansion in powers of $m_\pi/\Lambda_{\text{QCD}}$. In particular, quark mass dependent

short-distance contact operators (such as the D term) discussed in the above text do not appear in standard phenomenological interactions.

Since we are not presently able to obtain reliable values for the ${}^7\text{Li}$ binding energies, the ${}^7\text{Li}$ abundances we compute are not very meaningful and were not used to put constraints on the quark mass variations. Future advances in the nuclear pionless effective theory may change this and allow us to address the ‘lithium problem’ as a signal of quark mass variation.

Finally, it should be pointed out that, in models of physics beyond the standard model, the value of the quark masses are derived quantities and their variations may well be correlated with other quantities. In particular, it may seem unnatural to expect the masses of different quark flavors to vary together, unless this variation is being driven by a change in the Higgs vacuum expectation value. If that is the case, a change in the

quark masses will be correlated with changes in the vector boson masses, changing the strength of strong interactions at low energies. The effect of those changes on BBN can easily be tracked in a manner similar to what was done in this paper. We plan to consider BBN bounds on the Higgs vacuum expectation value change in a future presentation.

ACKNOWLEDGMENTS

We thank T. Cohen for discussions. P.B. was supported by the US Department of Energy under Grant No. DE-FG02-93ER-40762. The work of TL was performed under the auspices of the US Department of Energy by Lawrence Livermore National Laboratory under Contract DE-AC52-07NA27344 and the UNEDF SciDAC grant DE-FC02-07ER41457. L.P. was supported by the Department of Energy under Grant Number DE-FG02-00ER41132.

-
- [1] W. J. Marciano, *Phys. Rev. Lett.* **52**, 489 (1984).
 [2] J.-P. Uzan, *Rev. Mod. Phys.* **75**, 403 (2003).
 [3] J. P. Kneller and G. C. McLaughlin, *Phys. Rev. D* **68**, 103508 (2003).
 [4] V. F. Dmitriev, V. V. Flambaum, and J. K. Webb, *Phys. Rev. D* **69**, 063506 (2004).
 [5] A. Coc, N. J. Nunes, K. A. Olive, J.-P. Uzan, and E. Vangioni, *Phys. Rev. D* **76**, 023511 (2007).
 [6] V. V. Flambaum and E. V. Shuryak, *Phys. Rev. D* **67**, 083507 (2003).
 [7] V. F. Dmitriev and V. V. Flambaum, *Phys. Rev. D* **67**, 063513 (2003).
 [8] V. V. Flambaum and R. B. Wiringa, *Phys. Rev. C* **76**, 054002 (2007).
 [9] J. C. Berengut, V. V. Flambaum, and V. F. Dmitriev, *Phys. Lett. B* **683**, 114 (2010).
 [10] N. Chamoun, S. J. Landau, M. E. Mosquera, and H. Vucetich, *J. Phys. G* **34**, 163 (2007).
 [11] S. J. Landau, M. E. Mosquera, and H. Vucetich, *Astrophys. J.* **637**, 38 (2006).
 [12] C. M. Muller, G. Schafer, and C. Wetterich, *Phys. Rev. D* **70**, 083504 (2004).
 [13] V. V. Flambaum and E. V. Shuryak, *Phys. Rev. D* **65**, 103503 (2002).
 [14] X. Calmet and H. Fritzsch, *Eur. Phys. J. C* **24**, 639 (2002).
 [15] T. Dent and M. Fairbairn, *Nucl. Phys. B* **653**, 256 (2003).
 [16] A. Walker-Loud *et al.*, *Phys. Rev. D* **79**, 054502 (2009).
 [17] A. Walker-Loud, PoS **LATTICE2008**, 005 (2008).
 [18] S. R. Beane, P. F. Bedaque, M. J. Savage, and U. van Kolck, *Nucl. Phys. A* **700**, 377 (2002).
 [19] L. Platter, H. W. Hammer, and U.-G. Meißner, *Phys. Lett. B* **607**, 254 (2005).
 [20] J. Kirscher, H. W. Griesshammer, D. Shukla, and H. M. Hofmann, *Eur. Phys. J. A* **44**, 239 (2010).
 [21] S. R. Beane and M. J. Savage, *Nucl. Phys. A* **717**, 91 (2003).
 [22] E. Epelbaum, U.-G. Meißner, and W. Glöckle, *Nucl. Phys. A* **714**, 535 (2003).
 [23] S. R. Beane, P. F. Bedaque, P. F. Bedaque, K. Orginos, and M. J. Savage, *Phys. Rev. Lett.* **97**, 012001 (2006).
 [24] E. Braaten and H. W. Hammer, *Phys. Rev. Lett.* **91**, 102002 (2003).
 [25] E. Epelbaum, H.-W. Hammer, U.-G. Meißner, and A. Nogga, *Eur. Phys. J. C* **48**, 169 (2006).
 [26] H.-W. Hammer, D. R. Phillips, and L. Platter, *Eur. Phys. J. A* **32**, 335 (2007).
 [27] G. Rupak, *Nucl. Phys. A* **678**, 405 (2000).
 [28] M. Fukugita and T. Yanagida, *Physics of Neutrinos* (Springer, Berlin, 2003), p. 593.
 [29] V. Bernard, N. Kaiser, and U.-G. Meißner, *Int. J. Mod. Phys. E* **4**, 193 (1995).
 [30] J. Gasser and H. Leutwyler, *Ann. Phys.* **158**, 142 (1984).
 [31] S. R. Beane, K. Orginos, and M. J. Savage, *Nucl. Phys. B* **768**, 38 (2007).
 [32] J. Gasser and H. Leutwyler, *Phys. Rep.* **87**, 77 (1982).
 [33] R. V. Wagoner, *Astrophys. J.* **179**, 343 (1973).
 [34] L. Kawano, *Astrophys. J.*, 343, FERMLAB-PUB-92-004-A.
 [35] [<http://www-thphys.physics.ox.ac.uk/people/SubirSarkar/bbn.html>].
 [36] P. Hunt and S. Sarkar, *Phys. Rev. D* **76**, 123504 (2007).
 [37] J. Dunkley *et al.* (WMAP Collaboration), *Astrophys. J. Suppl.* **180**, 306 (2009).
 [38] K. Nakamura *et al.* (Particle Data Group Collaboration), *J. Phys. G* **37**, 075021 (2010).
 [39] J.-W. Chen, T.-K. Lee, C. P. Liu, and Y.-S. Liu, (2010), [arXiv:1012.0453](https://arxiv.org/abs/1012.0453).